Discontinuity lines in rectangular superconductors with intrinsic and extrinsic anisotropies

Th. Schuster and H. Kuhn
Max-Planck-Institut für Metallforschung, Institut für Physik, Postfach 800665, D-70506 Stuttgart, Germany

M. V. Indenbom*
Institut de Génie Atomique, Ecole Polytechnique Fédérale de Lausanne, CH-1015 Lausanne, Switzerland
(Received 16 June 1995)

Magneto-optical investigations of the flux distributions in the critical state of a c-axis-oriented square $YBa_2Cu_3O_{7-\delta}$ thin film with an extrinsic anisotropy induced by an in-plane magnetic field are presented. The dependence of the anisotropy ratio of the critical currents on the orientation of the in-plane field with respect to the direction of current flow is determined. The results are compared with flux distributions in a rectangular $DyBa_2Cu_3O_{7-\delta}$ single crystal with a microstructural anisotropy induced by the introduction of oblique linear defects. For the intrinsic anisotropy the flux is found to penetrate parallel to the inclination direction of the pins even if the flux motion is then not parallel to the Lorentz force exerted by the shielding currents. The angular distribution of the critical currents in general is different from the elliptic distribution, which was found for the extrinsic anisotropy.

I. INTRODUCTION

The main problem for finite superconductors (in particular thickness $\ll$ lateral extension) is that the shielding currents flow in the entire sample surface immediately when a transverse magnetic field is applied.[1,2] Moreover, the shielding currents change their magnitude and direction during magnetization.[3,4] To avoid these problems we investigate samples in the critical state, i.e., fully penetrated by magnetic flux. In the isotropic case the current takes then the critical value j_c everywhere in the specimen and flows parallel to the sample edges. In rectangular superconductors the streamlines of the current have to bend sharply and thus discontinuity lines (d lines) of the current flow occur.[1,5]

In anisotropic superconductors one can define two main directions with maximum and minimum j_c, respectively. The directions of the shielding currents in general do not coincide with the directions of these critical currents. As will be shown in this paper, the origin of the anisotropy is crucial for the behavior of the shielding currents, when the anisotropy axes are at an arbitrary orientation to the sample edges (which define the direction of the shielding currents) and we have to distinguish between intrinsic and extrinsic anisotropies. An intrinsic anisotropy is due to the microstructure of the sample and the preferred direction of flux motion may be caused by, e.g., the Cu-O planes,[6–9] by planar defects such as twin boundaries,[10–15] or by artificially introduced oriented pinning sites, e.g., inclined columnar defects.[16,17] An extrinsic anisotropy of flux penetration is induced into an isotropic sample by a special experimental arrangement, e.g., application of an in-plane magnetic field.[18]

In this paper we present magneto-optical investigations of the flux distributions in the critical state of a c-axis-oriented $YBa_2Cu_3O_{7-\delta}$ (YBCO) thin film of square shape with an extrinsic anisotropy and a $DyBa_2Cu_3O_{7-\delta}$ (DBCO) single crystal with an intrinsic anisotropy. The obtained flux patterns are interpreted by considering the observed d lines. Thus we are able to point out basic differences in the flux-penetration behavior and the critical-current distributions between both anisotropies.

The paper is organized as follows. In Sec. II the critical state in type-II superconductors and the properties of the current-discontinuity lines are outlined. Our magneto-optical method and the sample preparation are described in Sec. III. In Sec. IV our experimental results are presented and Sec. V summarizes our results.

II. CRITICAL STATE IN RECTANGULAR SUPERCONDUCTORS

In this paper we restrict our considerations to the Bean[19] approximation j_c = const. For $j_c = f(H)$ one obtains qualitatively the same results.[20] If the sample is in the critical state, i.e., fully penetrated by magnetic flux, the current density in the entire specimen takes its maximum possible value $|\mathbf{j}| = j_c$. In addition, the current density has to satisfy the continuity condition div $\mathbf{j} = 0$ and has to flow parallel to the surfaces. For superconductors with rectangular cross section, it follows from these conditions that the current stream lines have sharp bends; this is a characteristic feature of vector fields with constant modulus.[21] As discussed in the review by Campbell and Evetts,[1,5] these sharp bends form discontinuity lines (d lines) which divide the superconductor into domains with uniform parallel current flow; see Figs. 1 and 2. One distinguishes two types of d lines:[22] at d^+ lines the orientation of $\mathbf{j}_c$ changes discontinuously but the magnitude of j_c remains the same. At d^- lines the magnitude of j_c changes, e.g., at the specimen surface or at inner boundaries where regions of different j_c meet. At such boundaries the current lines have to bend sharply in order to satisfy the condition of continuous current flow. In superconductors which are isotropic in the x-y plane, the d^+ lines run along the bisection

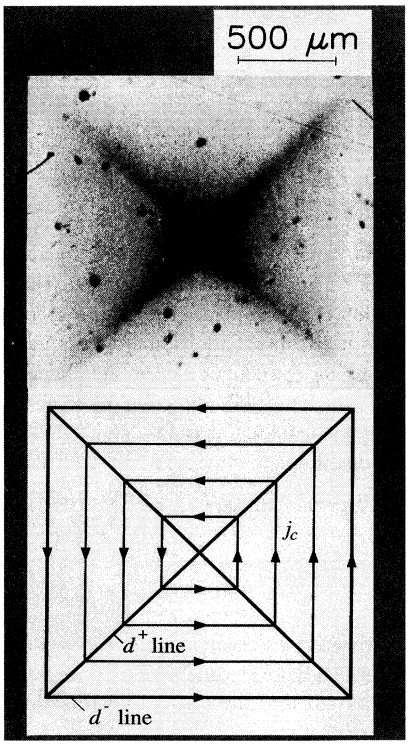

FIG. 1. Isotropic flux (top) and current (bottom) pattern in a square YBCO thin film in the critical state. The magnetic field H_a is applied perpendicular to the sample surface. The temperature is $T = 50$ K and $\mu_0 H_a = 151$ mT. The flux distribution was visualized using a ferrimagnetic iron-garnet indicator.

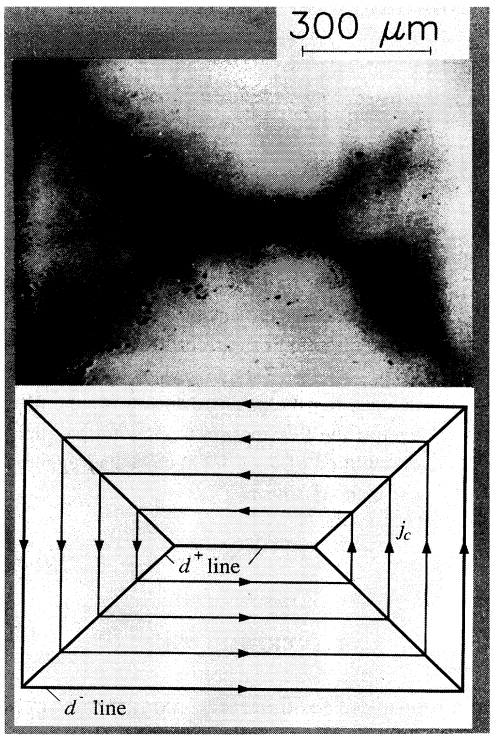

FIG. 2. The same as Fig. 1 but for a rectangular YBCO crystal at $T = 5$ K and $\mu_0 H_a = 512$ mT.

lines starting from the sample corners and on a section of the middle line parallel to the longer side as shown in Fig. 1 for a square and Fig. 2 for a rectangle.

Characteristic features of the d^+ and d^- lines are the following.

(1) Whereas the d^- lines occur at internal and external boundaries of the sample, the d^+ lines separate the superconductor into regions with homogeneous current flow and are determined by the shape of the sample.

(2) Flux lines cannot cross the d^+ lines since during increase of the applied magnetic field the flux lines move towards the d^+ lines from both sides. In contrast, the d^- lines can be crossed by flux, e.g., when flux lines penetrate from the surface. When the current does not flow parallel to the d^- line, a strong flux motion is directed along the d^- line.

(3) The electric field E is largest at the d^- lines, whereas we have $E=0$ at the d^+ lines.[4]

(4) The d^+ and the d^- lines do not change their position during lowering or reversing of the external magnetic field, although the magneto-optically detected intensities of the d^+ and d^- lines are reversed in the remanent state.

In thin type-II superconductors these d^+ and d^- lines are clearly seen because of the logarithmic infinity of B_z at the sample surface.[22]

III. EXPERIMENTS

A. Magneto-optical technique

We visualize the magnetic field distribution of a superconductor by the magneto-optical Faraday effect. The flux penetration is imaged by detecting the rotation of the polarization plane when linearly polarized light passes a magneto-optically active layer exposed to the magnetic field of the underlying superconductor. From flux-free regions the light is reflected without rotation of the polarization plane; this light thus cannot pass an analyzer which is set in a crossed position with respect to the polarizer. In this way the Shubnikov phase (with a flux-line lattice) will be imaged as bright areas, whereas the flux-free Meissner phase remains dark. For the experiments presented in this paper we used EuSe thin films and ferrimagnetic iron-garnet films with an in-plane anisotropy as magneto-optical indicators.

The EuSe thin films were deposited by electron-beam evaporation directly onto the sample surface, which was coated before with an aluminum layer (thickness about 200 nm), in order to enhance its reflectivity.[23] This technique allows flux distributions to be observed directly with a spatial resolution of about 1 μm in a temperature range of 5 K $\leqslant T \leqslant$ 20 K. The lower temperature boundary is given by the cryostat used, the upper limit is imposed by the temperature dependence of the Verdet constant of the europium chalcogenides, which leads to very low rotation angles at higher temperatures.[24] However, flux distributions at temperatures T

>20 K can be visualized indirectly by a special procedure during which the flux distribution obtained at a given temperature is observed after cooling the sample down to 5 K. This technique gives the correct flux patterns because j_c becomes larger when the temperature is decreased; therefore, the sample at lower temperatures enters an undercritical state, i.e., the flux distribution is not changed.[25]

The iron garnet film with a thickness of about 3.5 μm was grown by liquid phase epitaxy onto a gallium-gadolinium substrate (commercial firm Gamma Scientific Production, Russia).[26] This kind of indicator allows the flux penetration into high-temperature superconducting samples to be observed directly in the whole temperature range of superconductivity with a magnetic sensitivity of about 1 mT and a spatial resolution of about 4 μm.

The external magnetic field is generated by a copper solenoid coil, which is cooled with liquid nitrogen and produces a maximum field of 0.55 T. The observations were performed in the optical cryostat described in Refs. 23 and 27. All images can be observed directly via the microscope or may be transferred to an image processing system for analyzing.[28] The image processing system allows one to determine the grey level pixel by pixel along a user-defined line.

B. Sample preparation and irradiation

We use DBCO single crystals prepared as described in Ref. 29. The crystal dimensions are about 500 × 500 × 15 μm^3 and $T_c \approx 88$ K as measured by the Meissner effect using SQUID magnetometry. All crystals have a distinct twin structure which was revealed by polarized light microscopy. The EuSe thin film was deposited on all single crystals before the irradiation. To reduce scatter of the sample properties all crystals were investigated magneto-optically before and after the irradiation.

Inclined columnar defects were introduced by irradiation with 0.9 GeV Pb ions to a fluence $\phi t = 1.41 \times 10^{11}$ ions/cm^2 at GANIL (Caen, France). The samples were glued on copper sample holders and mounted at an angle $\varphi = 45°$ between the ion beam and the surface normal. The heavy ion irradiation lowers the critical temperature T_c by about 2 K at the fluence used.

The rectangular YBCO single crystal was produced at the Universität Karlsruhe by the method described in Ref. 30.

The c-axis-oriented YBCO thin films were produced at the Max-Planck-Institut für Festkörperforschung in Stuttgart, Germany, by a laser-ablation technique.[31] The thin films were patterned chemically to squares with a lateral length of 1.5 mm.

IV. RESULTS AND DISCUSSION

A. Extrinsic critical-current anisotropy

An anisotropy of flux penetration in a flat type-II superconductor in a transverse field can be induced by applying an in-plane magnetic field.[18] In this section we present investigations of such an anisotropy of the current and magnetic field distribution in the remanent state of a square YBCO thin film. The constant in-plane magnetic field of $\mu_0 H_i = 175$ mT is generated by a permanent magnet which can be rotated. The sample was cooled down to $T = 80$ K $< T_c$ in an applied in-plane magnetic field which is indicated by the white arrows in Fig. 3. Then a transverse magnetic field of $\mu_0 H_a = 200$ mT was applied to reach the critical state and was subsequently reduced to 0. The remanent state allows us to evaluate the obtained flux distributions very easily because the d^+ lines, which separate the domains of constant uniform current flow, are then clearly visible as bright lines; see Fig. 3. The presence of an in-plane field changes the observed flux distribution and the current distribution drastically from the in-plane-field free situation shown in Fig. 1.[18] Now the d^+ lines starting from the corners of the square do no longer run along the diagonals (the bisection lines of the corners) and therefore a central d^+ line occurs in the square, which shows that the critical current is no longer isotropic.[32] The flux lines generated by H_a penetrate the square more easily from the two edges which run perpendicular to H_i than from the edges parallel to H_i. This is due to the Lorentz force density $\mathbf{f} = \mathbf{j} \times \mathbf{B}_i$ which tilts the in-plane vortices more strongly into the transverse (out of plane) direction when the angle between $\mathbf{j}$ (induced by H_a) and $\mathbf{B}_i$ is close to 90°.

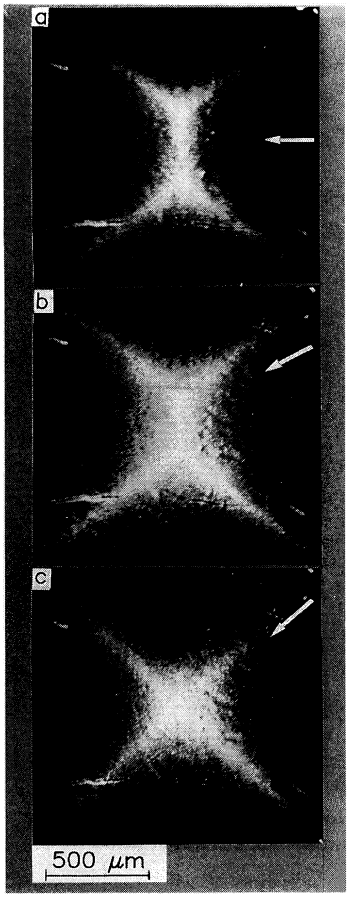

FIG. 3. Flux distribution with an in-plane magnetic field $\mu_0 H_i = 175$ mT for three different angles α. (a) $\alpha = 0°$; (b) 25°; (c) 45°. The direction of H_i is indicated by the white arrows. The flux distributions were visualized using a ferrimagnetic iron-garnet indicator.

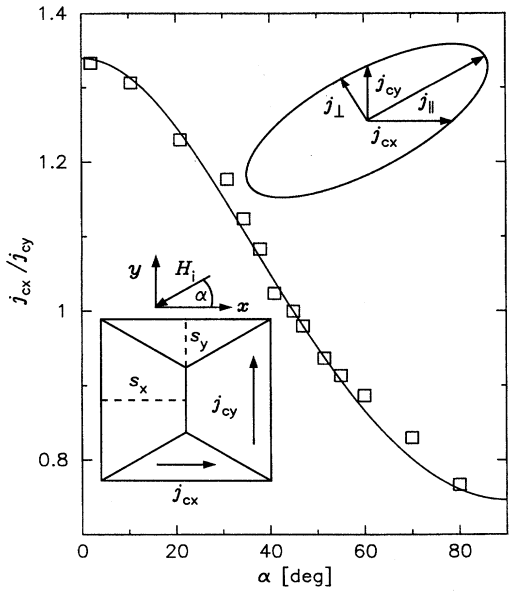

FIG. 4. Angular dependence of the ratio $\eta(\alpha)$ measured from magneto-optical images as presented in Fig. 3 (□) and calculated from Eq. (1) (solid line). The lower inset shows the directions of the critical currents and the orientation of H_i at an arbitrary angle α. The ratio of the distances s_x/s_y gives the ratio of the critical currents j_{cx}/j_{cy}. The upper inset shows the change of the critical currents when the semiaxes $j_{\parallel}$ and $j_{\perp}$ of the current ellipse are inclined to the directions of current flow by an arbitrary angle α.

Therefore the critical current density parallel to H_i is larger than the one perpendicular to H_i. The ratio of the two critical current densities j_{cx}/j_{cy} can be determined with high accuracy by measuring the distances s_x and s_y from the middle of the sample edges to the central d^+ line; see the lower inset in Fig. 4. From div $\mathbf{j} = 0$ one then finds $j_{cx}/j_{cy}=s_x/s_y$. In Fig. 3(a) we have $H_i \| x$ and we can determine the ratio $\eta_0=j_{\parallel}/j_{\perp} = 1.34$ of the critical current densities flowing along the left and right and the upper and lower edges, respectively. The ratio η changes if H_i is rotated by an angle α away from the direction in Fig. 3(a); see the d^+ line structures in Figs. 3(b) and 3(c).

While for an isotropic planar critical-current distribution the current vectors (in the critical state) define a circle of radius j_c, the extrinsic anisotropy induced by H_i distorts this circle perpendicular and parallel to the in-plane field such that the current vectors form an ellipse with the long semiaxis oriented parallel to H_i. This can be easily understood if one considers the Lorentz force density f_L exerted on an arbitrary oriented vortex by the current j_{cx}. The vortex is at an angle α to j_{cx} in the specimen plane and to the surface normal at an angle θ. Since for a critical current density $j_c=f_p/\Phi_0$, where f_p is the elementary pinning force density and Φ_0 the flux quantum, we have $f_L=-f_p$, it follows from the Lorentz force density $\mathbf{f}_L=-\Phi_0[\mathbf{l}\times\mathbf{j}_a]$ ($\mathbf{l}$ is a unit vector along the vortex) that $j_c=j_a(\cos^2\theta+\sin^2\theta\,\sin^2\alpha)^{1/2}$. For $H_i \| x$, see Fig. 3(a), the critical current densities, which flow always parallel to the sample edges, are given by the semiaxes parallel to x, $j_{\parallel}$, and parallel to y, $j_{\perp}$. When H_i is rotated by an angle α, the semiaxes of the current ellipse no longer coincide with the directions of current flow; see the upper inset in Fig. 4. The critical currents, therefore, change their magnitude which can be expressed by the components parallel to the semiaxes of the ellipse as $j_{cx}=(j_{\parallel}^2\cos^2\alpha+j_{\perp}^2\sin^2\alpha)^{1/2}$ and $j_{cy}=(j_{\parallel}^2\sin^2\alpha+j_{\perp}^2\cos^2\alpha)^{1/2}$; for the definitions of the currents see both insets in Fig. 4. The ratio $\eta=j_{cx}/j_{cy}$ is thus

$$\eta(\alpha)=\frac{j_{cx}}{j_{cy}}=\left[\frac{\eta_0^2\cos^2\alpha+\sin^2\alpha}{\cos^2\alpha+\eta_0^2\sin^2\alpha}\right]^{1/2}, \qquad (1)$$

with $\eta_0=1/\cos\theta$, which depends on the ratio H_a/H_i. The angular dependence of η, Eq. (1), is plotted in Fig. 4 as a solid line and is in excellent agreement with the experimentally determined values (□). At $\alpha = 45°$ [Fig. 3(c)] one has $\eta = 1$ and the critical-current distribution is isotropic; however, the modulus of $j_c=j_{cx}=j_{cy}$ may differ from the critical current density without an in-plane field. From Eq. (1) one can see that $\eta(\alpha)$ is fully determined when it is measured in the range $0\leq\alpha\leq45°$.

B. Intrinsic critical-current anisotropy

An intrinsic critical-current anisotropy was induced in a DBCO single crystal by introduction of oblique linear pins. As discussed recently[16] the anisotropy is caused by the different geometrical arrangements of flux lines and pins in the direction of vortex motion parallel and perpendicular to the inclination direction of the linear pins. Parallel flux-line motion is induced by the critical current density $j_{\perp}$, which flows perpendicular to the inclination plane of the pins, and can proceed easier than perpendicular flux-line motion induced by $j_{\parallel}$. Therefore we have $j_{\parallel}>j_{\perp}$.

In the experiment the inclination plane was at an angle $\alpha=27°$ to the longer sample edge; see Fig. 5(a). The direction of shielding currents is determined by the sample geometry since they flow parallel to the edges, whereas the critical currents $j_{\parallel}$ and $j_{\perp}$ are defined along the anisotropy axes which are at the angle α to the sample edges. Now an interesting phenomenon occurs. The flux motion does no longer proceed perpendicular to the edges as in the isotropic case or with an extrinsic anisotropy, but preferentially parallel to the inclination plane as indicated by the black arrow in Fig. 5(b). This leads to the formation of broad d^+ lines starting from the upper left and lower right sample corner, which are aligned with the inclination plane. The d^+ lines to the upper right and lower left corners tighten. The double Y of the d^+-line structure is oriented perpendicular (in the isotropic case parallel) to the longer crystal edge.

Because the shielding currents, j_1 and j_2 in Fig. 5(c), flow parallel to the sample edges, the axes $j_{\parallel}$ and $j_{\perp}$ of the critical-current anisotropy do not coincide with the directions of current flow. The angular dependence of the currents is unknown in this case, but we can surely exclude an elliptic dependence, which was found for the extrinsic anisotropy in the previous section. The Lorentz force on the flux lines exerted by the shielding currents is directed perpendicular to the edges. However, the flux lines avoid the motion parallel

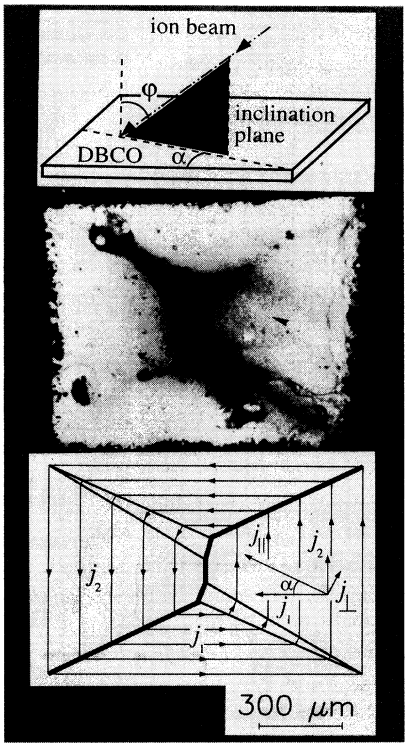

FIG. 5. (a) Sketch of the geometric arrangement of the samples and the ion beam. (b) Magneto-optically measured flux distribution in an obliquely irradiated DBCO single crystal at $T = 50$ K using a ferrimagnetic iron-garnet indicator. The external field $\mu_0 H_a = 512$ mT is applied perpendicular to the surface. The black arrow indicates the direction of flux motion parallel to the inclination plane of the introduced linear pins. (c) Current pattern for an arbitrary orientation of the anisotropy axes $j_\parallel$ and $j_\perp$ to the crystal edges. The shielding currents $j_1 > j_2$ flow parallel to the sample edges.

to the Lorentz force and move more easily parallel to the inclination plane of the pins. Therefore, the shielding currents parallel to the sample edges always exceed the lowest critical current density perpendicular to the inclination plane when $\alpha \neq 0$. In general both shielding currents j_1 and j_2 are different; from the magneto-optically determined flux pattern we obtain $j_1/j_2 = 2$.

At the d^+ lines, at which the shielding current changes from the larger j_1 to the lower j_2 [see Fig. 5(c)], the component $j_1 \sin\alpha$ perpendicular to the inclination plane can exceed $j_\perp$. In this case the d^+ line splits into two d^+ lines, which form a new region. Since this newly established domain is bounded by two d^+ lines which start from the same corner the current flow is there no longer directed parallel to the sample edges. The flux lines cannot penetrate into this area and the current there is not limited by flux motion.

If the inclination plane of the linear defects introduced by oblique heavy-ion irradiation were directed parallel to a sample edge, we would have obtained a similar field distribution in our nearly rectangular DBCO crystal as in the square with applied in-plane field [Fig. 3(a)].[17]

This similarity applies also for other intrinsic anisotropies induced by the microstructure of the sample, such as twin boundaries or the Cu-O planes, when the crystal c axis lies in the plane of observation.

V. CONCLUSION

In this paper we have pointed out differences in the flux penetration into samples with intrinsic and extrinsic critical-current anisotropies. We investigated magneto-optically the critical state in a square YBCO thin film, into which an extrinsic anisotropy was introduced by an in-plane magnetic field, and in a DBCO single crystal with an intrinsic anisotropy induced by oblique linear defects, which were introduced by heavy-ion bombardment. In the case of an extrinsic anisotropy we found an angular dependence of the critical currents in form of an ellipse with the semiaxes parallel and perpendicular to the direction of the in-plane field. For the intrinsic anisotropy the angular dependence of the critical currents is more complicated, i.e., it should exhibit a sharp toothlike minimum in the direction of preferential vortex motion. The magnetic flux was found to penetrate always along the preferred direction parallel to the inclination plane of the linear pins. For arbitrary orientations of the anisotropy axes with respect to the sample edges the flux motion is thus not directed perpendicular to the current flow. The d-line structure may become unstable when the component $j_1 \sin\alpha$ exceeds the lowest critical current $j_\perp$ in the sample. The d^+ line then splits into two d^+ lines. This can happen only at those d^+ lines starting from the corners, which are along the direction of preferential vortex motion. This is in contrast to the current pattern proposed by Campbell and Evetts in Refs. 1 and 5, where the splitting occurs at all d^+ lines starting from the corners.

In the case of an extrinsic anisotropy the splitting of the d^+ lines at arbitrary angles α, which was predicted by Campbell and Evetts,[1,5] does not occur, because in this situation the critical current densities parallel to the semiaxes of the ellipse are not present in the sample.

From our experiments follows for all integral magnetization measurements, e.g., SQUID (superconducting quantum interference device), VSM (vibrating sample magnetometer), or torque measurements, that the orientation of the sample with respect to the applied field has to be very carefully accounted for. Especially for angular dependent measurements, the magnetic moment is strongly influenced by the anisotropic current distribution, which is induced by an arbitrary orientation of the magnetic field with respect to the sample. Moreover, the interpretation of the magnetization data is even more complicated if intrinsic anisotropies, e.g., due to twin boundaries or the Cu-O planes, influence the current distribution in the sample.

ACKNOWLEDGMENTS

We wish to thank Professor H. Kronmüller (Max-Planck-Institut für Metallforschung, Stuttgart) for his constant interest in this work, M. Leghissa and G. Kreiselmeyer (Univer-

sität Erlangen) for the performance of the irradiation, M. Kläser (Universität Karlsruhe) for the rectangular YBCO single crystal, and H.-U. Habermeier (Max-Planck-Institut für Festkörperforschung, Stuttgart) for the YBCO thin film. Part of this work was supported by the Bundesministerium für Bildung, Wissenschaft, Forschung und Technologie (Grant No. 13N6510). This is gratefully acknowledged. One of us (M.V.I.) is grateful to Fond National Suisse de la Recherche Scientifique (FNPN30 Grant No. 4030-32794) and the Alexander-von-Humboldt Stiftung.

*Permanent address: Institute of Solid State Physics, Russian Academy of Sciences, Chernogolovka, 142432 Moscow, Russian Federation.

[1] A. M. Campbell and J. E. Evetts, *Critical Currents in Superconductors* (Taylor & Francis, London, 1972).

[2] H. Theuss, A. Forkl, and H. Kronmüller, Physica (Amsterdam) C **190**, 345 (1992).

[3] E. H. Brandt, Phys. Rev. Lett. **74**, 3025 (1995); (unpublished).

[4] Th. Schuster, H. Kuhn, E. H. Brandt, M. V. Indenbom, M. Kläser, G. Müller-Vogt, H.-U. Habermeier, H. Kronmüller, and A. Forkl, Phys. Rev. B **52**, 10 375 (1995).

[5] A. M. Campbell and J. E. Evetts, in *Concise Encyclopedia of Magnetic & Superconducting Materials*, edited by J. Evetts (Pergamon, Oxford, 1992), p. 95.

[6] L. Schimmele, H. Kronmüller, and H. Teichler, Phys. Status Solidi B **147**, 361 (1988).

[7] M. Tachiki and S. Takahashi, Solid State Commun. **70**, 291 (1989).

[8] B. Roas, L. Schultz, and G. Saemann-Ischenko, Phys. Rev. Lett. **64**, 479 (1990).

[9] Th. Schuster, M. R. Koblischka, H. Kuhn, M. Glücker, B. Ludescher, and H. Kronmüller, J. Appl. Phys. **74**, 3307 (1993).

[10] Th. Schuster, M. R. Koblischka, B. Ludescher, and H. Kronmüller, J. Appl. Phys. **72**, 1478 (1992).

[11] A. I. Belyaeva, S. V. Voitsenya, V. P. Yur'ev, M. A. Obolenskii, and A. V. Bondarenko, Superconductivity **5**, 1406 (1992).

[12] C. A. Duran, P. L. Gammel, R. Wolf, V. J. Fratello, D. J. Bishop, J. P. Rice, and D. M. Ginsberg, Nature **357**, 474 (1992).

[13] V. K. Vlasko-Vlasov, M. V. Indenbom, and A. A. Polyanskii, in *The Real Structure of High-T_c Superconductors*, edited by V. Sh. Shekhtman, Springer Series in Materials Science Vol. 23 (Springer, Berlin, 1993), pp. 111–144.

[14] A. I. Belyaeva, S. V. Voitsenya, V. P. Yuriyev, M. A. Obolenskii, and A. V. Bondarenko, Solid State Commun. **55**, 427 (1993).

[15] M. Turchinskaya, D. L. Kaiser, F. M. Gayle, A. J. Shapiro, A. Roytburd, V. Vlasko-Vlasov, A. Polyanskii, and V. Nikitenko, Physica (Amsterdam) C **216**, 205 (1993).

[16] Th. Schuster, M. V. Indenbom, H. Kuhn, H. Kronmüller, M. Leghissa, and G. Kreiselmeyer, Phys. Rev. B **50**, 9499 (1994).

[17] Th. Schuster, H. Kuhn, M. Indenbom, M. Leghissa, M. Kraus, and M. Konczykowski, Phys. Rev. B **51**, 16 358 (1995).

[18] M. V. Indenbom, A. Forkl, B. Ludescher, H. Kronmüller, H.-U. Habermeier, B. Leibold, G. D'Anna, T. W. Li, P. H. Kes, and A. A. Menovsky, Physica (Amsterdam) C **226**, 325 (1994).

[19] C. P. Bean, Rev. Mod. Phys. **36**, 31 (1964); J. Appl. Phys. **41**, 2482 (1970).

[20] Th. Schuster, H. Kuhn, E. H. Brandt, M. V. Indenbom, M. R. Koblischka, and M. Konczykowski, Phys. Rev. B **50**, 16 684 (1994).

[21] H. A. M. van den Berg, J. Appl. Phys. **60**, 1104 (1986).

[22] Th. Schuster, M. V. Indenbom, M. R. Koblischka, H. Kuhn, and H. Kronmüller, Phys. Rev. B **49**, 3443 (1994).

[23] Th. Schuster, M. R. Koblischka, N. Moser, B. Ludescher, and H. Kronmüller, Cryogenics **31**, 811 (1991).

[24] R. P. Huebener, *Magnetic Flux Structures in Superconductors* (Springer, New York, 1979).

[25] M. V. Indenbom, Th. Schuster, M. R. Koblischka, A. Forkl, H. Kronmüller, L. A. Dorosinskii, V. K. Vlasko-Vlasov, A. A. Polyanskii, R. L. Prozorov, and V. I. Nikitenko, Physica (Amsterdam) C **209**, 259 (1993).

[26] L. A. Dorosinskii, M. V. Indenbom, V. I. Nikitenko, Yu. A. Ossip'yan, A. A. Polyanskii, and V. K. Vlasko-Vlasov, Physica (Amsterdam) C **203**, 149 (1992).

[27] K.-H. Greubel, E. Gmelin, N. Moser, Ch. Mensing, and L. Walz, Cryogenics **30** (Suppl.), 457 (1990).

[28] M. R. Koblischka, N. Moser, B. Gegenheimer, and H. Kronmüller, Physica (Amsterdam) C **166**, 36 (1990).

[29] C. Thomsen, M. Cardona, B. Gegenheimer, R. Liu, and R. Simon, Phys. Rev. B **37**, 9860 (1988).

[30] A. Erb, T. Traulsen, and G. Müller-Vogt, J. Cryst. Growth **137**, 487 (1994).

[31] H.-U. Habermeier, Eur. J. Solid State Inorg. Chem. **28**, 619 (1991).

[32] E. M. Gyorgy, R. B. van Dover, K. A. Jackson, L. F. Schneemeyer, and J. V. Waszack, Appl. Phys. Lett. **55**, 283 (1989); F. M. Sauerzopf, A. P. Wiesinger, and H. W. Weber, Cryogenics **30**, 650 (1990).

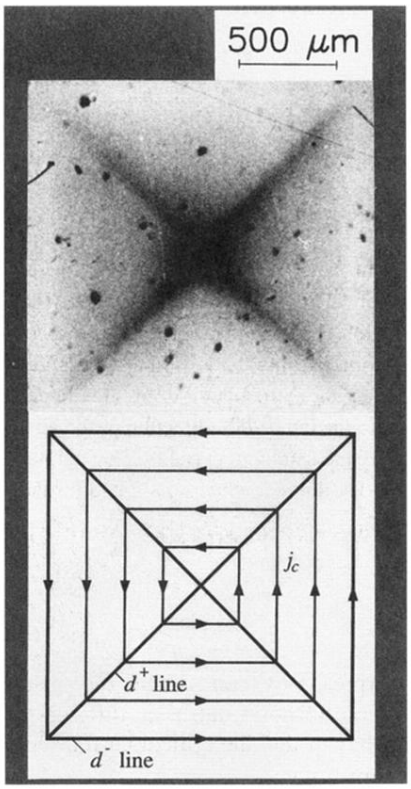

FIG. 1. Isotropic flux (top) and current (bottom) pattern in a square YBCO thin film in the critical state. The magnetic field H_a is applied perpendicular to the sample surface. The temperature is $T = 50$ K and $\mu_0 H_a = 151$ mT. The flux distribution was visualized using a ferrimagnetic iron-garnet indicator.

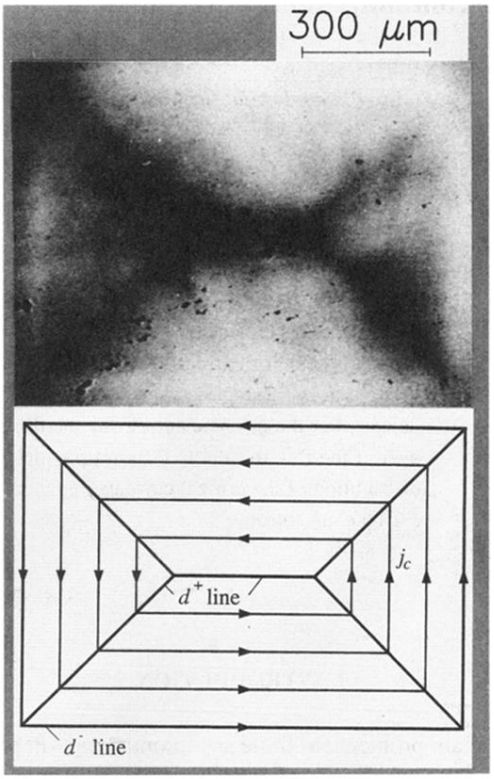

FIG. 2. The same as Fig. 1 but for a rectangular YBCO crystal at $T = 5$ K and $\mu_0 H_a = 512$ mT.

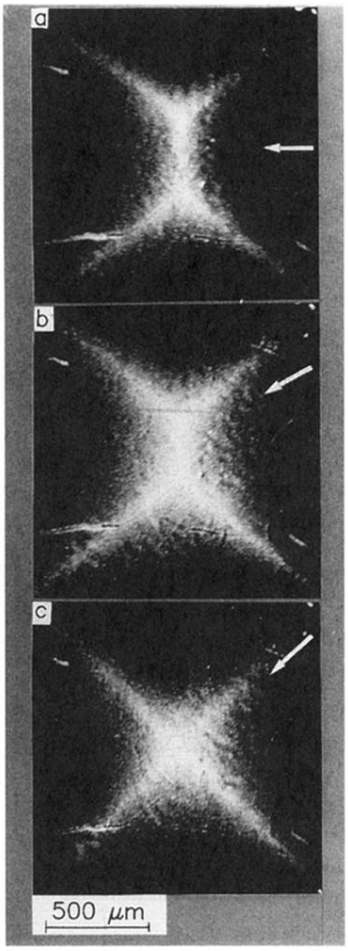

FIG. 3. Flux distribution with an in-plane magnetic field $\mu_0 H_i$ = 175 mT for three different angles α. (a) α = 0°; (b) 25°; (c) 45°. The direction of H_i is indicated by the white arrows. The flux distributions were visualized using a ferrimagnetic iron-garnet indicator.

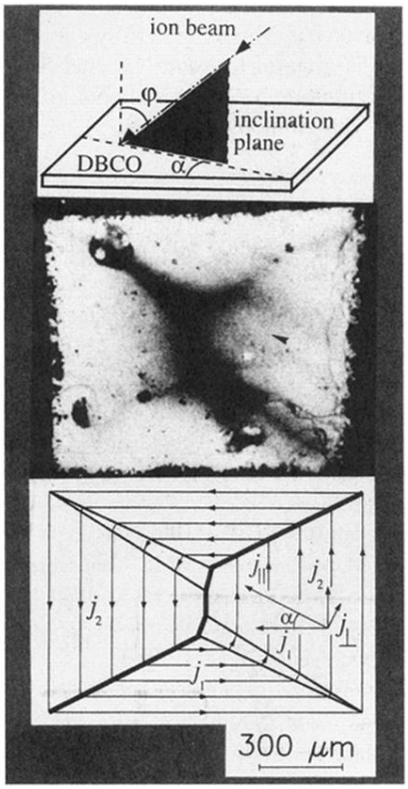

FIG. 5. (a) Sketch of the geometric arrangement of the samples and the ion beam. (b) Magneto-optically measured flux distribution in an obliquely irradiated DBCO single crystal at $T = 50$ K using a ferrimagnetic iron-garnet indicator. The external field $\mu_0 H_a = 512$ mT is applied perpendicular to the surface. The black arrow indicates the direction of flux motion parallel to the inclination plane of the introduced linear pins. (c) Current pattern for an arbitrary orientation of the anisotropy axes $j_{\parallel}$ and $j_{\perp}$ to the crystal edges. The shielding currents $j_1 > j_2$ flow parallel to the sample edges.